

Magnetic Properties of Grain Boundaries and Precipitates in Nanocrystalline Ni and Ni-Cu Alloys

H. Wolf¹, Z. Guan¹, St. Lauer¹, H. Natter², M. Schmelzer²,
R. Hempelmann² and Th. Wichert¹

¹ Technische Physik, Universität des Saarlandes, DE-66041 Saarbrücken, Germany

² Physikalische Chemie, Universität des Saarlandes, DE-66041 Saarbrücken, Germany

Keywords: Electrodeposition, Nanocrystalline, Ni, Ni-Cu, PAC

Abstract

Nanocrystalline Ni and Ni-Cu alloys are investigated on atomic scale by perturbed $\gamma\gamma$ angular correlation spectroscopy, X-ray diffraction, and energy dispersive X-ray spectroscopy. The samples are produced by pulsed electrodeposition and, at the same time, doped with radioactive ^{111}In probe atoms. The investigations in nanocrystalline Ni show a new local magnetic field, which is attributed to magnetically slightly perturbed lattice sites near the grain boundaries. In $\text{Ni}_{0.50}\text{Cu}_{0.50}$ alloys the presence of the local magnetic field of crystalline Ni is used as indicator for an inhomogeneous composition of these alloys. The homogeneity of this alloys is improved if during electrodeposition the temperature is increased, the current density reduced, and, especially, if saccharin is added to the electrolyte.

Introduction

The production of nanocrystalline materials by pulsed electrodeposition (PED) offers some advantages compared to inert gas condensation or ball-milling, because high purity material is obtained at a high production rate [1,2,3]. In addition, the density of the deposited material reaches that of polycrystalline material and, therefore, no compaction procedure is necessary. Nanocrystalline Ni is investigated in order to get a fundamental understanding of ferromagnetism in nanocrystals [4,5] as well as with respect to industrial applications [6]. With help of PED pure metals as well as intermetallic compounds, such as Ni-Cu alloys, can be deposited as nanocrystalline materials [1,3]. The experimental investigations presented here are performed by perturbed $\gamma\gamma$ angular correlation spectroscopy (PAC) using radioactive $^{111}\text{In}/^{111}\text{Cd}$ probe atoms. With help of PAC the magnetic properties of nanocrystalline Ni and the composition and homogeneity of Ni-Cu alloys are investigated on atomic scale.

Experimental details

The composition of the electrolyte and the used parameters during the deposition of Ni and the Ni-Cu alloys are listed in Table 1. The samples were doped with ^{111}In by adding $^{111}\text{InCl}_3$ to the electrolyte. As a reference to the Ni samples produced by PED a polycrystalline Ni foil was doped with ^{111}In by diffusion at 1330 K under vacuum.

In the present PAC experiments, the local magnetic field is measured at the site of the probe atom $^{111}\text{In}/^{111}\text{Cd}$. The data yield information about local magnetic properties of crystallites and interfaces and about the formation of new ferromagnetic phases. The probe ^{111}In decays to an excited level of its daughter isotope ^{111}Cd , followed by the emission of a γ - γ cascade including the intermediate $I = 5/2$ nuclear level with a lifetime of $\tau = 123$ ns. The emission probability of the second quantum γ_2 with respect to γ_1 is spatially anisotropic because of the conservation of angular

Table 1: Composition of the electrolyte, temperature, current density, on- and off-times of the current pulses, used for the deposition of nanocrystalline Ni and Ni-Cu alloys.

sample	electrolyte	T	j	t _{on}	t _{off}
Ni #A	NiSO ₄ (40g/l), K,Na-tartrate (120g/l), NH ₄ Cl (40g/l)	36.5 °C	0.5 A/cm ²	2 ms	48 ms
Ni #B	NiSO ₄ (40g/l), K,Na-tartrate (120g/l), NH ₄ Cl (40g/l), saccharin (2g/l)	36.5 °C	0.13 A/cm ²	1 ms	49 ms
Ni-Cu #A	CuSO ₄ (6g/l), NiSO ₄ (80g/l), Na-citrate (100g/l)	36.5 °C	0.5 A/cm ²	1 ms	49 ms
Ni-Cu #B	CuSO ₄ (6g/l), NiSO ₄ (80g/l), Na-citrate (100g/l)	15 - 70 °C	0.1 A/cm ²	2 ms	48 ms
Ni-Cu #C	CuSO ₄ (6g/l), NiSO ₄ (80g/l), Na-citrate (100g/l)	36.5 °C	0.1 - 0.3 A/cm ²	2 ms	48 ms
Ni-Cu #D	CuSO ₄ (6g/l), NiSO ₄ (80g/l), Na-citrate (100g/l), saccharin (2g/l)	36.5 °C	0.1 - 0.3 A/cm ²	2 ms	48 ms

momentum. The hyperfine interaction of the local magnetic field (\mathbf{B}_{loc}) with the nuclear magnetic moment μ of the $I = 5/2$ level effects a modulation of the emission probability of γ_2 , which is detected at a fixed angle θ with respect to γ_1 . The modulation is governed by the Larmor frequency ω_L , from which the magnetic field at the site of the ^{111}Cd nucleus is obtained by the relation:

$$g \cdot \mu_N \cdot \mathbf{B}_{loc} = \hbar \cdot \omega_L \quad (\text{Eq. 1})$$

Here, μ_N is the nuclear magneton and $g = -0.3062$ the nuclear g-factor of the $I = 5/2$ level of ^{111}Cd . The PAC time spectrum $R(t)$ is described by

$$R(t) = A_2 \cdot \left[f \cdot \left(s_0 + s_1 \cos(\omega_L t) \cdot \exp\left(-\frac{(\Delta\omega_L t)^2}{2}\right) + s_2 \cos(2\omega_L t) \cdot \exp\left(-\frac{(2\Delta\omega_L t)^2}{2}\right) \right) + (1-f) \right] \quad (\text{Eq. 2})$$

whereby t reflects the time passed between the emission of the two γ -quanta. From the $R(t)$ spectrum the two frequencies ω_L and $2\omega_L$ are extracted yielding \mathbf{B}_{loc} (Eq. 1). The amplitude f of the modulation reflects the fraction of probe atoms residing in an environment that produces a particular non-zero magnetic field \mathbf{B}_{loc} . The fraction of probe atoms exposed to a zero field is denoted by $(1-f)$. In the case of different environments, characterised by different values of \mathbf{B}_{loc} , f is split into different fractions f_i , whereby each fraction is associated with its own characteristic Larmor frequency. In general, a distribution about the modulation frequencies ($\Delta\omega_L$) is present, which is caused by slight perturbations in the neighbourhood of the probe atom. For the present experiments a Gaussian distribution is assumed. A more detailed description of PAC spectroscopy is found elsewhere [7,8].

The XRD experiments were performed at a Siemens D5000 θ - θ spectrometer using the K_α radiation of Cu. The grain size of the nanocrystalline Ni samples was determined by analyzing the broadening of the diffraction peaks according to the method of Warren-Averbach [9]. In case of the Ni-Cu alloys, the lattice constant determined by XRD gives access to the composition of these samples [3]. Additionally, the composition was measured by energy dispersive X-ray spectroscopy (EDX).

Results and discussion

1.) Nanocrystalline Ni

Samples of nanocrystalline Ni were produced by pulsed electrodeposition and, at the same time, doped with the radioactive ^{111}In probe atoms. For the Ni #A samples none and for the Ni #B samples 2g/l saccharin was added to the electrolyte. The XRD analysis yields a mean grain size of 40 nm for sample Ni #A, and 19 nm for Ni #B. The PAC spectra for sample Ni #A and the polycrystalline reference sample are displayed in Fig. 1. The modulation field arises from the local magnetic field of ferromagnetic Ni and the data for Ni #A show besides the sharp Larmor frequency of $\omega_L^0 = 97.6$ Mrad/s known from polycrystalline Ni [10], a second, new frequency (Fig. 1a). The new frequency is shifted to a lower value $\omega_L^1 = 95.8$ Mrad/s and is significantly broadened by $\Delta\omega_L^1 = 6$ Mrad/s. The fractions of probe atoms, which measure the frequencies ω_L^0 and ω_L^1 are about $f_0 = 57\%$ and $f_1 = 43\%$, respectively. The PAC results obtained for the nanocrystalline samples Ni #A and Ni #B and for the polycrystalline Ni are summarised in Table 2. The formation of the new component f_1 with the shifted frequency ω_L^1 is obviously correlated with the grain size in the nanometer range and, additionally, the shift $\omega_L^1 - \omega_L^0$ and the broadening $\Delta\omega_L^1$ increase with decreasing grain size. These observations along with the fact that the component f_1 disappears when grain growth occurs by annealing the sample at a temperature above 423 K [11], suggest that the new component f_1 is connected with lattice sites in the outer region of a grain and f_0 to sites in the core of a grain. Assuming a statistical distribution of the ^{111}In atoms over the whole sample and using the fractions f_1 and the grain size measured by XRD, the width of the outer region of the grains is estimated to be 3 - 4 nm [11,12]. These observations are consistent with investigations performed by Mößbauer spectroscopy on nanocrystalline Ni and Fe [13].

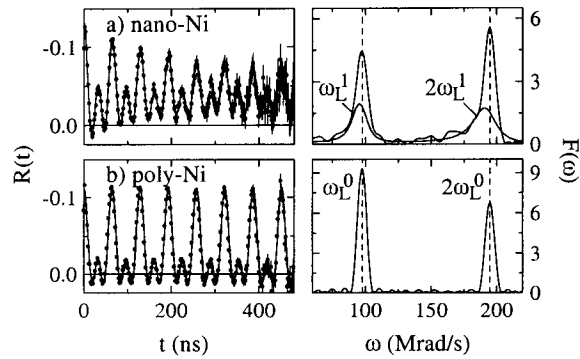


Fig. 1: PAC spectra measured (a) in nanocrystalline (Ni #A) and (b) in polycrystalline Ni in zero external field at 295 K.

Table 2: The fraction f , the Larmor frequency ω_L , and the width of the frequency distribution $\Delta\omega_L$ about ω_L for both components of magnetic dipole interaction detected at Ni samples with different grain sizes.

grain size	f_0	ω_L^0	$\Delta\omega_L^0$	f_1	ω_L^1	$\Delta\omega_L^1$
19 nm (Ni #B)	33 %	98.0(4) Mrad/s	0 Mrad/s	67 %	94.0(6) Mrad/s	10 Mrad/s
40 nm (Ni #A)	57 %	97.7(4) Mrad/s	0 Mrad/s	43 %	95.8(6) Mrad/s	6 Mrad/s
polycrystalline	100 %	97.6(2) Mrad/s	0 Mrad/s	-	-	-

The incorporation of the isotope ^{111}In into nanocrystalline Ni upon diffusion was investigated by PAC as a function of the diffusion temperature for samples deposited by PED. The incorporation of ^{111}In at substitutional lattice sites is recognised by the well known Larmor frequency of $\omega_L = 97.6$ Mrad/s [10]. The PAC results obtained on nanocrystalline and, for comparison, on polycrystalline Ni are plotted in Fig. 2. Following diffusion of ^{111}In into nanocrystalline Ni at $T_{\text{diff}} = 670$ K, already $f_{\text{Ni}} = 9\%$ of the probe atoms are incorporated on substitutional lattice sites within the Ni crystallites. The fraction f_{Ni} increases, when the sample is subsequently annealed at

770 K and 870 K. In contrast, no ^{111}In atoms reside on substitutional sites in polycrystalline Ni following diffusion at 670 K, even after subsequent annealing at 770 K. A temperature of 870 K is required, to incorporate 10 % of the ^{111}In atoms on lattice sites within the crystallites. Since grain growth in nanocrystalline Ni is known to start at 423 K [3], it is concluded that the incorporation of ^{111}In atoms into the nanocrystallites is favoured by the grain growth. In the nanocrystalline samples, additional signals are observed at about $\omega = 25$ Mrad/s and $\omega = 64$ Mrad/s (Fig. 2), which are not yet identified. It is assumed that these signals belong to sites within the grain boundaries; their identification will be subject of new experiments.

2.) Ni-Cu alloys

Ni-Cu samples were deposited by PED and investigated by PAC and XRD. The composition was determined by EDX to 50 at% Ni and 50 at% Cu. The XRD spectrum shows the fcc structure of Ni-Cu alloys. The $\langle 111 \rangle$ -diffraction peak for sample Ni-Cu #A is plotted in Fig. 3. The position of this peak is located at a scattering angle that is located between those known for pure Cu and Ni, in agreement with the composition determined by EDX. The diffraction peak is significantly broadened as compared with a diffraction peak of a perfect crystal and it shows an asymmetric shape. The PAC spectrum of this sample, recorded directly after the deposition by PED shows a distribution of frequencies, centred at about $\bar{\omega} = 50$ Mrad/s and, in addition, the sharp Larmor frequency of $\omega_L = 97.6$ Mrad/s of crystalline Ni (Fig. 4a). Obviously, the Ni-Cu sample is not homogenous after deposition and contains crystallites of pure Ni, in which

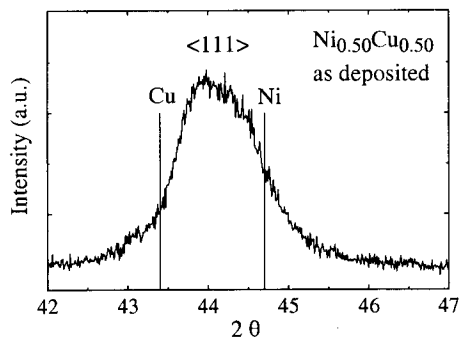


Fig. 3: XRD data of sample Ni-Cu #A after deposition. The $\langle 111 \rangle$ -reflex is shown to be located between the corresponding scattering angles of pure Cu and pure Ni.

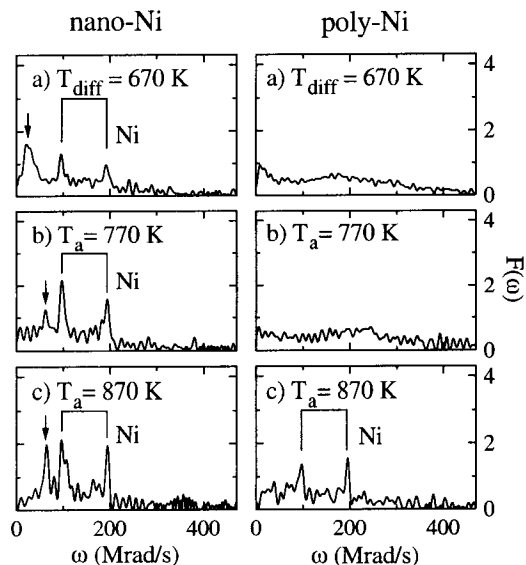


Fig. 2: Fourier transforms of PAC spectra measured in (a) nanocrystalline (Ni #B) and in (b) polycrystalline Ni after diffusion of ^{111}In at 670 K, and after annealing at 770 K and 870 K. In case of nanocrystalline Ni, the observation of new signals is marked by an arrow.

the sharp Larmor frequency of $\omega_L = 97.6$ Mrad/s of crystalline Ni (Fig. 4a). Obviously, the Ni-Cu sample is not homogenous after deposition and contains crystallites of pure Ni, in which $f_{\text{Ni}} = 20$ % of the probe atoms are located. After annealing the sample at 473 K, the fraction of ^{111}In in pure Ni crystallites increases slightly to 23 %, before it starts to decrease at $T_a = 673$ K. At a temperature of $T_a = 873$ K, finally, the Ni crystallites are no longer observed (i.e. $f_{\text{Ni}} < 2$ %) and only the frequency distribution about $\bar{\omega} = 50$ Mrad/s is present. Such a frequency distribution is expected for a disordered Ni-Cu solid solution and is caused by the different arrangements of Ni and Cu atoms in the neighbourhood of the ^{111}In probe atoms. The above mentioned Ni precipitates are not easily visible, if at all, in the XRD analysis in Fig. 3, although the asymmetric shape of the diffraction peak seems to be caused by the presence of Ni precipitates. Since the shape of the diffraction peaks is affected by the

presence of Ni crystallites in the Ni-Cu samples, the determination of the grain size by XRD is no more reliable. Thus, a determination of the grain size of the Ni-Cu samples could not be performed, up to now.

The influence of the temperature of the electrolyte, the current density, and the addition of saccharin to the electrolyte on the homogeneity of Ni-Cu alloys is visible in the Fourier transforms $F(\omega)$ shown in Fig. 5. The temperature was varied between 15 °C and 70 °C keeping the current density constant at 0.1 A/cm² (Ni-Cu #B). The current density was varied between 0.1 and 0.3 A/cm² keeping the temperature constant at 36.5 °C, whereby one series of samples was deposited without (Ni-Cu #C) and a second with addition of saccharin to the electrolyte (Ni-Cu #D). The fraction of Ni crystallites is reduced by increasing the temperature at a constant current density (left

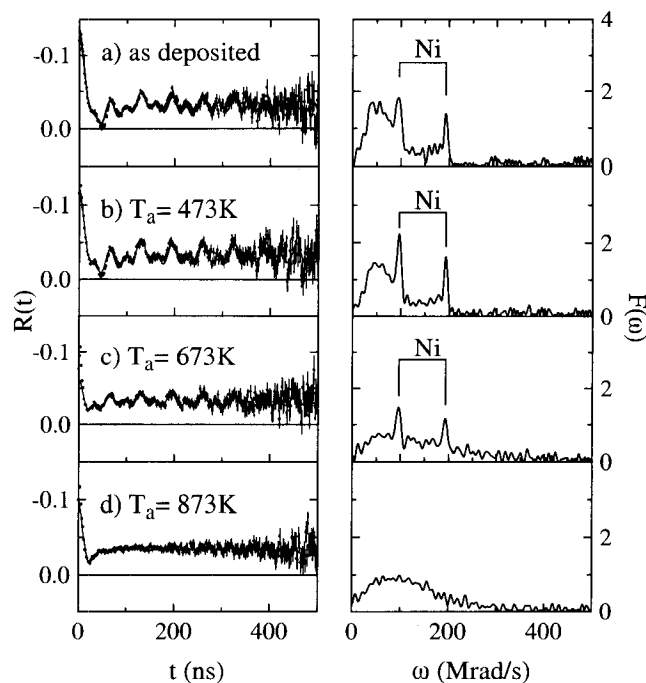


Fig. 4: PAC spectra measured in sample Ni-Cu #A (a) after deposition, and (b-d) after annealing at temperatures between 473 K and 873 K.

column) and by decreasing the current density at constant temperature (centre and right columns). Obviously, the Ni-Cu alloy becomes more homogeneous at lower current densities and at higher temperatures. These conditions during deposition, however, are known to be correlated with an increasing grain size [3]. Adding saccharin to the electrolyte (2 g/l), no Ni crystallites are observed by PAC at any current density, but only a frequency distribution as it is expected for a disordered Ni_{0.50}Cu_{0.50} solid solution (right column in Fig 5). The addition of saccharin is obviously advantageous for producing homogeneous Ni-Cu alloys and, at the same time, is known to reduce the grain size during deposition [3].

Summary

In nanocrystalline Ni samples, having grain sizes of 19 nm or 40 nm, the PAC experiments show two different local magnetic fields. One component is known from polycrystalline Ni and is attributed to sites in the core of the crystallites. The second component is characterised by a slightly smaller Larmor frequency and a finite frequency distribution and is attributed to lattice sites in the outer part of the crystallites. The width of this so-called magnetic boundary is estimated to 3 - 4 nm and, thereby, significantly larger than the crystallographic boundary .

The PAC investigations at Ni_{0.50}Cu_{0.50} alloys show the formation of pure Ni crystallites during the PED process, which are not identified by XRD. The Ni-Cu alloys become more homogeneous, if the temperature of the electrolyte is increased or the current density is reduced, both processes being at the expense of an increase of the grain size [3]. The homogeneity of the Ni-Cu alloys is improved and at the same time the grain size reduced, if saccharin is added to the electrolyte.

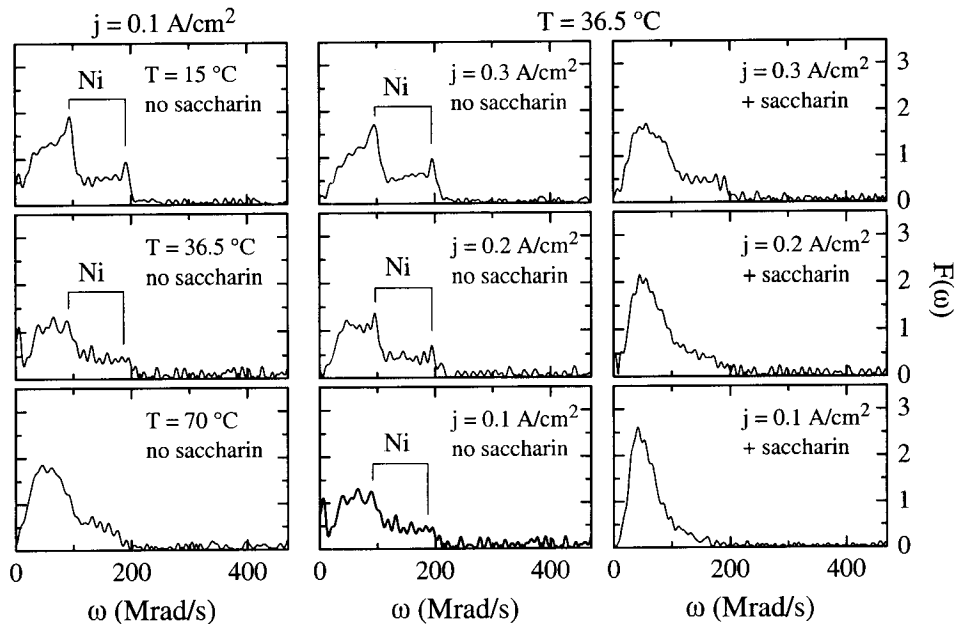


Fig. 5: Fourier transforms $F(\omega)$ of PAC spectra measured in different $Ni_{0.50}Cu_{0.50}$ alloys, which are deposited via PED under different conditions (temperature, current density, content of saccharin).

Acknowledgements

We thank Dr. H. Ehrhardt and M. Schuler (Lehrstuhl Prof. Birringer, Saarbrücken) for the XRD and EDX analysis of the Ni-Cu samples. The financial support by the Deutsche Forschungsgemeinschaft (SFB 277) is thankfully acknowledged.

References

- 1.) D. Osmola, E. Renaud, U. Erb, L. Wong, G. Palumbo, and K.T. Aust, *Mat. Res. Soc. Symp. Proc.* **286** (1993), p. 191
- 2.) H. Natter, M. Schmelzer, S. Janßen, and R. Hempelmann, *Ber. Bunsenges. Phys. Chem* **101** (1997), p. 1706
- 3.) H. Natter, M. Schmelzer, and R. Hempelmann, *J. Mater. Res.* **13** (1998), p. 1186
- 4.) H. Kisker, T. Gessmann, R. Würschum, H. Kronmüller, and H.-E. Schaefer, *Nanostruct. Mater.* **6** (1995), p. 925
- 5.) J.F. Löffler, J.P. Meier, B. Doudin, J.-P. Ansermet, and W. Wagner, *Phys. Rev.* **B57** (1998), p. 2915
- 6.) U. Erb, *Nanostruct. Mater.* **6** (1995), p. 533
- 7.) Th. Wichert and E. Recknagel, in *Microscopic Methods in Metals*, ed. U. Gonser, *Topics in Current Physics* **40** (1986), p. 317
- 8.) T. Butz, *Hyp.Int.* **52** (1989), p. 189
- 9.) B.E. Warren and B.L. Averbach, *J. Appl. Phys.* **21** (1950), p. 595, *J. Appl. Phys.* **23** (1952), p. 497
- 10.) D.A. Shirley, S.S. Rosenblum, and E. Matthias, *Phys. Rev.* **170** (1968), p. 363
- 11.) St. Lauer, Z. Guan, H. Wolf, H. Natter, M. Schmelzer, R. Hempelmann, and Th. Wichert *Nanostructured Materials*, in print
- 12.) St. Lauer, Z. Guan, H. Wolf, and Th. Wichert, *Hyperfine Interactions*, in print
- 13.) A. Krämer, J. Jing, and U. Gonser, *Hyp. Int.* **54** (1990), p. 591